

Ternary complex formation between AmtB, GlnZ and the nitrogenase regulatory enzyme DraG reveals a novel facet of nitrogen regulation in bacteria

Luciano F. Huergo,¹ Mike Merrick,²
Fábio O. Pedrosa,¹ Leda S. Chubatsu,¹
Luíza M. Araujo¹ and Emanuel M. Souza^{1*}

¹Department of Biochemistry and Molecular Biology,
Universidade Federal do Paraná, Curitiba-PR, Brazil.

²Department of Molecular Microbiology, John Innes
Centre, Norwich, UK.

Summary

Ammonium movement across biological membranes is facilitated by a class of ubiquitous channel proteins from the Amt/Rh family. Amt proteins have also been implicated in cellular responses to ammonium availability in many organisms. Ammonium sensing by Amt in bacteria is mediated by complex formation with cytosolic proteins of the P_{II} family. In this study we have characterized *in vitro* complex formation between the AmtB and P_{II} proteins (GlnB and GlnZ) from the diazotrophic plant-associative bacterium *Azospirillum brasilense*. AmtB–P_{II} complex formation only occurred in the presence of adenine nucleotides and was sensitive to 2-oxoglutarate when Mg²⁺ and ATP were present, but not when ATP was substituted by ADP. We have also shown *in vitro* complex formation between GlnZ and the nitrogenase regulatory enzyme DraG, which was stimulated by ADP. The stoichiometry of this complex was 1:1 (DraG monomer : GlnZ trimer). We have previously reported that *in vivo* high levels of extracellular ammonium cause DraG to be sequestered to the cell membrane in an AmtB and GlnZ-dependent manner. We now report the reconstitution of a ternary complex involving AmtB, GlnZ and DraG *in vitro*. Sequestration of a regulatory protein by the membrane-bound AmtB–P_{II} complex defines a new regulatory role for Amt proteins in Prokaryotes.

Introduction

Ammonium is the preferential nitrogen source for most prokaryotes and its movement across biological mem-

branes is facilitated by a class of ubiquitous channel proteins. The ammonium transport (Amt) family comprises the Amt proteins found in Bacteria, Archaea, fungi and plants, and the related Rhesus proteins, which are found in animals from nematodes to man (Merrick *et al.*, 2006). In Bacteria, Archaea, fungi and plants the Amt proteins facilitate ammonium uptake when the extracellular ammonium levels are low. The 3D crystal structures of AmtB from *Escherichia coli* (Khademi *et al.* 2004; Zheng *et al.*, 2004) and the related Amt-1 from *Archeoglobus fulgidus* (Andrade *et al.* 2005a) are very similar. Both proteins are homotrimers in which each subunit spans the membrane 11 times generating a narrow channel within each monomer that is believed to conduct unprotonated ammonia (NH₃) (Winkler, 2006).

Nitrogen metabolism in bacteria is co-ordinated by a class of highly conserved and widely distributed signal transduction proteins from the P_{II} family (Arcondéguy *et al.*, 2001; Forchhammer, 2004). The P_{II} proteins from *E. coli* (GlnB and GlnK) have been subjected to detailed biochemical and structural investigation (Ninfa and Jiang, 2005). These proteins are homotrimers that form a compact barrel 30 Å high (Xu *et al.*, 2001) and, at the top of the barrel, each subunit extends a flexible region known as the T-loop (Xu *et al.*, 1998). In *E. coli*, and all Gram-negative bacteria studied so far, the T-loop can be modified by uridylylation of a conserved tyrosine residue (Tyr51), and this post-translational modification is regulated according to the cellular nitrogen status (Jiang *et al.*, 1998). P_{II} proteins can also bind up to three ATP and three 2-oxoglutarate (2-OG) molecules in a synergistic manner (Kamberov *et al.*, 1995; Forchhammer and Hedler, 1997). The ATP binding sites are located in the lateral clefts between the P_{II} subunits (Xu *et al.*, 2001). The 2-OG binding site has yet to be identified but it has been suggested that it may also be located in the lateral clefts in the vicinity of the ATP γ -phosphate (Xu *et al.*, 1998; Benelli *et al.*, 2002; Gruswitz *et al.*, 2007).

P_{II} proteins co-ordinate nitrogen metabolism through the regulation of transcriptional activators, key metabolic enzymes and membrane transporters (Forchhammer, 2004; Ninfa and Jiang, 2005). This regulation is achieved by direct protein–protein interaction and the ability of P_{II} proteins to interact with and regulate their targets can be

Accepted 18 October, 2007. *For correspondence. E-mail souzaem@ufpr.br; Tel. (+55) 41 3361 1667; Fax (+55) 41 3362 2042.

influenced by their uridylylation status and also by ATP and 2-OG levels (Ninfa and Jiang, 2005).

In a variety of bacteria it has been shown that, in response to elevated levels of extracellular ammonium, P_{II} proteins can be sequestered to the cell membrane in an AmtB-dependent manner (Coutts *et al.*, 2002; Detsch and Stulke, 2003; Strosser *et al.*, 2004; Huergo *et al.*, 2006a; Zhang *et al.*, 2006; Tremblay *et al.*, 2007; Wolfe *et al.*, 2007). In *E. coli* this phenomenon has been studied at the molecular level and AmtB and GlnK have been shown to form a trimer-to-trimer complex with a 1:1 stoichiometry (Durand and Merrick, 2006). Recently, the 3D crystal structure of the *E. coli* AmtB–GlnK complex, formed either *in vivo* or *in vitro*, was determined. The basis of the interaction is an intimate association of the T-loop of GlnK with the cytoplasmic vestibule of AmtB (Conroy *et al.*, 2007; Gruswitz *et al.*, 2007). Complex formation occurs only with de-uridylylated GlnK and is regulated by ATP and 2-OG levels (Durand and Merrick, 2006).

Besides their role in ammonium uptake, Amt proteins have also been implicated in cellular responses to extracellular ammonium availability in fungi (Lorenz and Heitman, 1998), slime moulds (Singleton *et al.*, 2006) and bacteria (Martin and Reinhold-Hurek, 2002; Yakunin and Hallenbeck, 2002; Wang *et al.*, 2005; Huergo *et al.*, 2006a; Zhang *et al.*, 2006). The physiological role of AmtB–GlnK complex formation in *E. coli* is to inactivate the channel. However, complex formation also reduces the cytoplasmic content of GlnK with potential physiological consequences (Coutts *et al.*, 2002) and our recent studies have suggested that the AmtB–P_{II} complex might target other regulatory proteins to the cell membrane (Huergo *et al.*, 2006a,b).

Some nitrogen-fixing bacteria can regulate nitrogenase activity post-translationally by ADP-ribosylation of dinitrogenase reductase (NifH) when conditions become unfavourable for nitrogen fixation, e.g. upon addition of ammonium to the extracellular medium. ADP-ribosylation is effected by the DraT enzyme and NifH can be reactivated by the DraG enzyme which cleaves the ADP-ribosyl group when the added ammonium is exhausted by cellular metabolism (Zhang *et al.*, 1997). We have previously shown that in *Azospirillum brasilense* DraG is targeted to the cell membrane after an ammonium shock in an AmtB and GlnZ-dependent manner (Huergo *et al.*, 2006a). A similar phenomenon was observed with DraG from *Rhodospirillum rubrum* (Wang *et al.*, 2005). Based on our *in vivo* studies we proposed a model for the regulation of DraG, in which DraG is inactivated through membrane sequestration by the formation of a ternary complex involving AmtB, GlnZ and DraG (Huergo *et al.*, 2006a,b). Here we present the *in vitro* reconstitution and characterization of such an AmtB–GlnZ–DraG ternary complex in *A. brasilense*. This report shows the formation of a ternary

complex between a regulatory enzyme and the AmtB–P_{II} complex and it identifies a potentially very significant new regulatory role for Amt proteins in Bacteria and Archaea.

Results

Purification of an N-terminal 6His-tagged version of A. brasilense AmtB

In order to purify *A. brasilense* AmtB, we constructed a plasmid (pLHPETHisAmtB) to express an N-terminally 6His-tagged AmtB under control of the T7 promoter. The 6His insertion was placed three residues after the predicted signal peptide cleavage site. The expression of this *amtB* allele in *A. brasilense* FAJ310 strain (*amtB::km*) restored ADP-ribosylation of the NifH protein after ammonium addition thus confirming that 6HisAmtB is functional *in vivo* (Fig. S1). The pLHPETHisAmtB plasmid was transferred to *E. coli* strain C43, cells were treated with IPTG, and HisAmtB expression and cellular localization were investigated by probing the whole-cell, cytoplasm or membrane fractions with a monoclonal anti-His antibody (GE-Healthcare) in Western blots (Fig. S2A). We observed three bands that reacted with anti-His with approximate molecular mass of 35 kDa, 70 kDa and 105 kDa. All these bands were predominantly located in the membrane fraction, suggesting that they could be monomeric, dimeric and trimeric forms of *A. brasilense* HisAmtB. All the Amt proteins studied so far, including AmtB from Archaea and Bacteria, show a trimeric structure and partially retain their trimeric structure on SDS-PAGE gels (Blakey *et al.*, 2002; Andrade *et al.*, 2005b). As we observe bands that might correspond to trimers of *A. brasilense* AmtB on SDS-PAGE gels (Fig. S2A), it is very likely that the AmtB protein from *A. brasilense* is also homotrimeric.

HisAmtB was purified from the membrane fraction of *E. coli* C43 cells carrying pLHPETHisAmtB (Fig. S2B). The monomeric form of AmtB was always predominant and the appearance of the 70 kDa and 105 kDa bands of purified HisAmtB varied from gel to gel. Bands corresponding to the putative monomeric and dimeric forms (Fig. S2B) were excised from the gel, digested with trypsin and subjected to mass spectrometry analysis by MALDI-TOF. Both bands yielded a similar spectra where only two peaks were detected (m/z of 1390.834, 2233.095 and 1391.375, 2233.693 for the upper and lower band respectively) these signals match two predicted peptides of *A. brasilense* AmtB (m/z 1390.6961, from amino acid residues 426 to 438 and 2233.0731, from 419 to 438, giving a protein coverage of 4.9%).

Influence of small effectors on HisAmtB–GlnB and HisAmtB–GlnZ complex formation in vitro

In vitro complex formation between *A. brasilense* AmtB and the P_{II} proteins GlnB and GlnZ were assayed by the

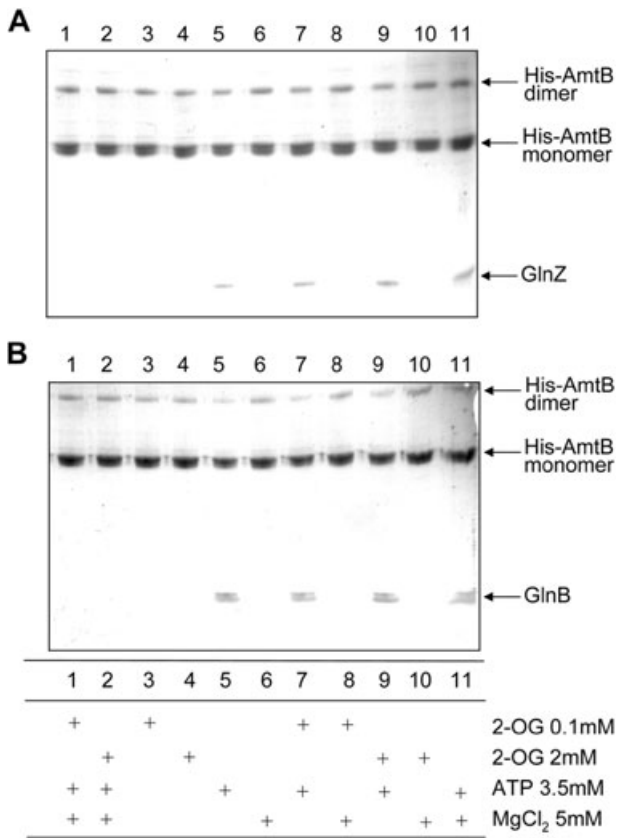


Fig. 1. *In vitro* formation of the AmtB-GlnB and AmtB-GlnZ complexes. Complex formation was assessed by coprecipitation using Ni²⁺ beads. Reactions were performed in buffer containing 50 mM Tris-HCl pH 8, 0.1 M NaCl, 0.05% LDAO, 10% glycerol, 20 mM imidazole in the presence (+) or absence of the effectors (MgCl₂, 2-OG or ATP) as indicated in the Table. Binding reactions were conducted in 500 μ l of buffer adding the purified proteins at concentrations of 0.15 μ M HisAmtB and 0.5 μ M GlnZ (A) or GlnB (B). The eluted fraction was subjected to SDS-PAGE, the gel was Coomassie blue stained. Arrows indicate the identified proteins.

coprecipitation technique (pull-down) using Ni²⁺ magnetic beads. Native GlnB or GlnZ were purified and mixed with HisAmtB protein in the presence of Ni²⁺ beads. After extensive washes, the proteins were eluted with 0.5 M imidazole. Control experiments indicated that GlnB and GlnZ do not bind to the beads (data not shown) and therefore, the presence of GlnB or GlnZ in the elution buffer after incubation with HisAmtB is indicative of interaction. Under specific conditions, both GlnB and GlnZ formed a complex with HisAmtB (Fig. 1). This confirms *in vivo* studies where both proteins were found membrane-associated in an AmtB-dependent manner after an ammonium shock (Huergo *et al.*, 2006a).

Several studies have shown that the ability of P_{II} proteins to interact with their targets can be influenced by the concentration of the P_{II} effectors, ATP and 2-OG. Formation of both the *A. brasilense* AmtB-GlnB and AmtB-GlnZ complexes responded similarly to the presence of effec-

tors (Fig. 1). In both cases formation of the complex required ATP (Fig. 1), as previously reported for the *E. coli* AmtB-GlnK complex (Durand and Merrick, 2006). However, whereas formation of the *E. coli* AmtB-GlnK complex was only inhibited by concentrations of 2-OG of 1 mM or greater, when MgCl₂ was present, the *A. brasilense* complex was inhibited at either 0.1 mM or 2 mM 2-OG, but also only in the presence of Mg²⁺ (Fig. 1A and B, compare lanes 1 and 7 or 2 and 9). Furthermore, inhibition of *A. brasilense* complex formation was still observed using very low concentrations of 2-OG such as 10 μ M (data not shown). Hence, we conclude that complex formation requires bound nucleotide and that the ATP-bound form of the complex is considerably more sensitive to 2-OG than the equivalent *E. coli* complex.

Recently, the crystal structure of the *E. coli* AmtB-GlnK complex, formed either *in vivo* (Conroy *et al.*, 2007) or *in vitro* (Gruswitz *et al.*, 2007), was determined. In both cases, the GlnK protein was surprisingly found to have three molecules of bound ADP, even though the *in vitro*-formed complex was crystallized in the presence of ATP. These results led us to study the effects of other adenine nucleotides on *A. brasilense* AmtB-GlnZ and AmtB-GlnB complex formation. Both ADP and AMP stimulated complex formation (Fig. 2A) but, in contrast to the situation with ATP (Fig. 1A), 2-OG, at concentrations up to 2 mM, did not affect AmtB-GlnZ complex formation in the presence of ADP and MgCl₂ (Fig. 2B). We therefore tested the ability of 2-OG to influence the dissociation of the complex.

The AmtB-GlnZ complex was linked to the Ni²⁺ beads, in the presence of ADP plus MgCl₂, and subjected to a wash step in buffer containing either ATP plus MgCl₂ or ADP plus MgCl₂ in the presence or absence of 2-OG at concentrations of 0.1 or 2 mM. The results, shown in Fig. 3, indicate that the AmtB-GlnZ complex is only sensitive to 2-OG in the presence of ATP, when increasing concentrations of 2-OG promote dissociation.

Following washes with 0.1 or 2 mM 2-OG plus ATP only 50% or 25%, respectively, of the GlnZ remained bound to HisAmtB, when compared with washing in the absence of 2-OG. In contrast, when ADP was present in the wash buffer the addition of 2-OG did not affect complex stability (Fig. 3).

In vitro complex formation between GlnZ and DraG is positively influenced by ADP

We have shown previously that *A. brasilense* GlnZ can form a complex with the nitrogenase regulatory enzyme DraG *in vivo* (Huergo *et al.*, 2006b). To further explore the role of GlnZ effectors in the *in vitro* formation of the GlnZ-DraG complex, we performed pull-down experiments with Ni²⁺ beads using an N-terminally His-tagged version of

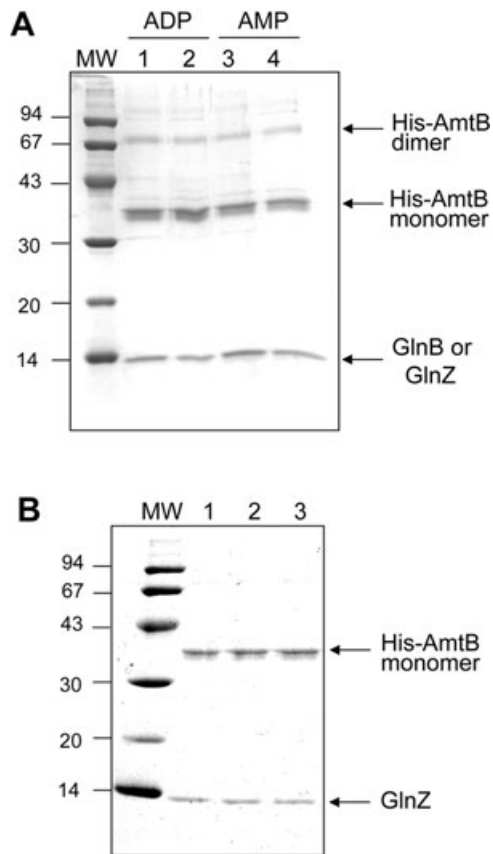


Fig. 2. ADP or AMP also allow AmtB–GlnB and AmtB–GlnZ complex formation and 2-OG does not affect AmtB–GlnZ complex formation in the presence of Mg-ADP.

A. Complex formation was carried out as described in Fig. 1 in the presence of 3.5 mM ADP or AMP as indicated. HisAmtB was incubated with GlnB (lanes 1 and 3) or GlnZ (lanes 2 and 4). B. Formation of the AmtB–GlnZ complex in buffer containing 3.5 mM ADP, 5 mM MgCl₂ in the absence of 2-OG (Lane 1) or in the presence of 0.1 mM (Lane 2) or 2 mM of 2-OG (Lane 3). Bound proteins eluted with imidazole 0.5 M were subjected to SDS-PAGE and the gel was Coomassie blue stained. Arrows indicate the identified proteins.

DraG (HisDraG) and native GlnZ. We have previously shown that the 6His-tagged version of DraG is active and normally regulated *in vivo* (Huergo *et al.*, 2005a; 2006b).

In vitro complex formation between HisDraG and either GlnZ or GlnB was therefore assayed by coprecipitation (pull-down) using Ni²⁺ magnetic beads. We added 5 mM of MnCl₂ to all buffer as Mn²⁺ is required for DraG activity *in vitro* (Saari *et al.*, 1984; Ljungstrom *et al.*, 1989). HisDraG was mixed with either GlnZ or GlnB in the presence or absence of ATP, ADP and 2-OG. The reactions were incubated with Ni²⁺ beads and, after extensive washing, the samples were eluted with 0.5 M of imidazole and analysed by SDS-PAGE.

We observed GlnZ copurification with HisDraG in the absence of nucleotides. Surprisingly, addition of ADP or ATP (3.5 mM) to the buffer had opposite effects: ATP

inhibited GlnZ–DraG interaction while ADP stimulated it (Fig. 4). The presence of 2-OG also negatively influenced complex formation (Fig. 4). Similar results were observed in the reverse experiment using HisGlnZ and native DraG (data not shown).

We did not detect GlnB copurification with HisDraG or DraG copurification with HisGlnB using the same conditions tested for GlnZ (data not shown), suggesting that DraG cannot interact with GlnB under our assay conditions, confirming previous *in vivo* data (Huergo *et al.*, 2006b).

We also tested the capacity of ATP and/or 2-OG to dissociate the DraG–GlnZ complex. The HisDraG–GlnZ complex was linked to Ni²⁺ beads in the presence of ADP and subjected to a wash step in buffer containing ADP, ADP plus 2-OG, ATP or ATP plus 2-OG. The results in Fig. 5 indicate that the His-DraG–GlnZ complex destabilized in the presence of 2-OG or ATP and that dissociation was substantially greater when 2-OG and ATP were used together.

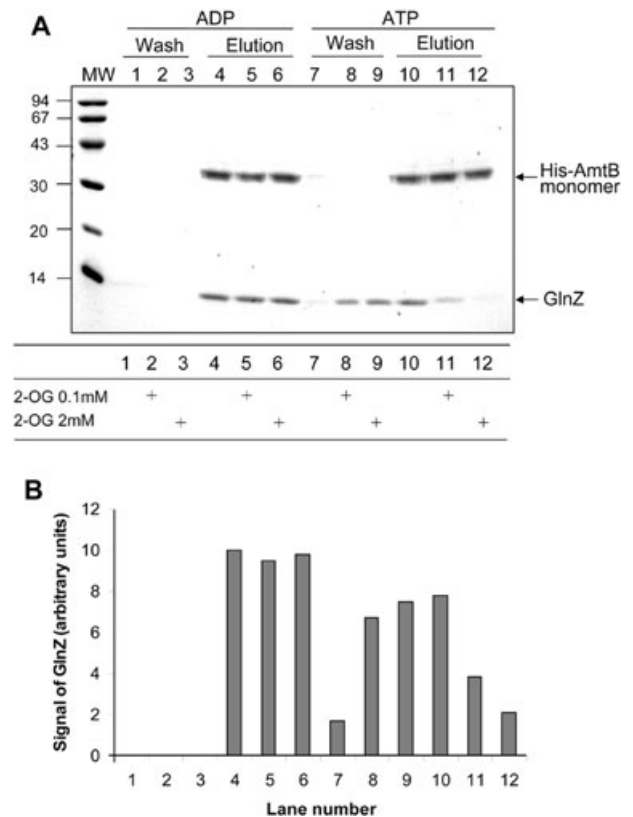


Fig. 3. Dissociation of the AmtB–GlnZ complex requires 2-OG and ATP. (A) The HisAmtB–GlnZ complex was immobilized on Ni²⁺ beads in buffer containing 3.5 mM ADP and 5 mM MgCl₂. Beads were washed (Wash) with buffer containing ADP or ATP and 2-OG at 0, 0.1 or 2 mM as indicated in the Table. Bound proteins were eluted with 0.5 M imidazole (Elution). The samples were submitted to SDS-PAGE, the gel was stained with Coomassie blue and the signal for GlnZ was quantified by densitometry (B). Arrows indicate the identified proteins.

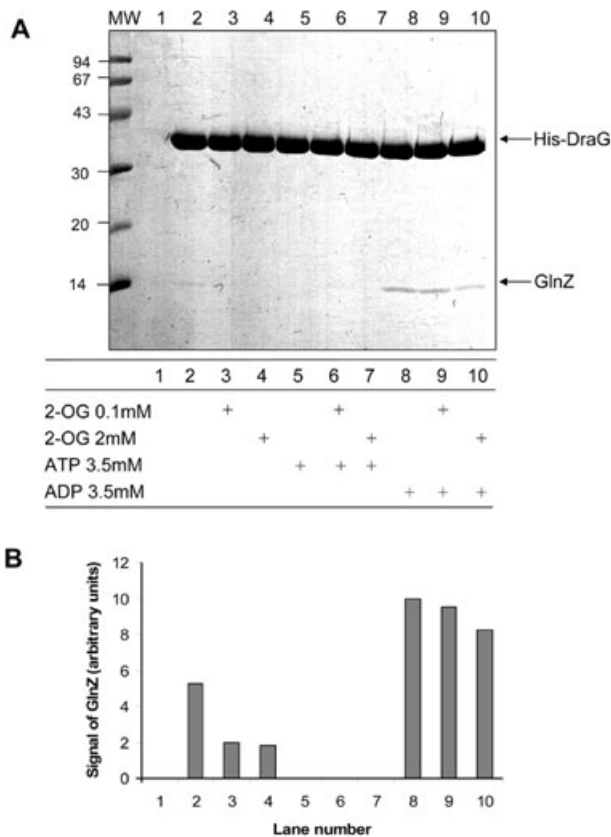


Fig. 4. *In vitro* DraG-GlnZ complex formation is stimulated by ADP. (A) The formation of the complexes was carried out by coprecipitation using Ni²⁺ beads. Reactions were performed in buffer containing 50 mM Tris-HCl pH 8, 0.1 M NaCl, 0.05% LDAO, 5 mM MnCl₂, 1 mM MgCl₂, 10% glycerol, 20 mM imidazole in the presence (+) or absence of the effectors (2-OG, ATP and ADP) as indicated in the Table. Binding reactions were conducted in 500 μl of buffer adding the purified proteins at a concentration of 1 μM HisDraG and 2 μM GlnZ. Lane 1 is a control where only GlnZ was added. The eluted fractions were subjected to SDS-PAGE, the gel was Coomassie blue stained and the signal for GlnZ was quantified by densitometry (B). Arrows indicate the identified proteins.

Gel filtration analysis of the DraG-GlnZ complex reveals a 1:1 monomer : trimer stoichiometry

In order to determine the stoichiometry of the DraG-GlnZ complex we performed gel filtration analysis of the purified native proteins alone or together in the presence of ADP. When applied separately to a Superose 12 gel filtration column, purified DraG was eluted as a single peak at 12.25 ml, corresponding to an apparent molecular mass of 34 kDa as determined by comparison with standard protein markers (Fig. 6). This molecular mass agrees well with that predicted for the DraG monomer (32 kDa) and with previous data on *R. rubrum* DraG (Saari *et al.*, 1984). When GlnZ was applied to the column, a single elution peak (12.09 ml) was detected, corresponding to 38 kDa which also agrees with the predicted molecular mass for a GlnZ trimer (37 kDa). When a mixture of DraG and GlnZ in

a 1:1 molar ratio (monomer to trimer respectively) was applied virtually all protein eluted in a single peak (10.95 ml), corresponding to 83 kDa (Fig. 6), which is close to the molecular weight (~69 kDa) predicted for a complex consisting of one monomer of DraG and one trimer of GlnZ. Moreover, quantification of the bands on an SDS-PAGE from the peak of the eluted complex revealed a molar ratio of monomeric DraG to trimeric GlnZ of 1:1 (Fig. 6, compare GlnZ : DraG ratio of the input with those of 11.0 ml and 11.5 ml fractions). The data suggest that the DraG-GlnZ complex consists of one DraG monomer bound to one GlnZ trimer.

In contrast to the gel filtration experiment, a substoichiometric recovery of GlnZ in comparison to His-DraG was obtained in the pull-down assays (compare the GlnZ : DraG ratio on the gels of Figs 4 and 6). A similar result was obtained when His-GlnZ was used to pull-down

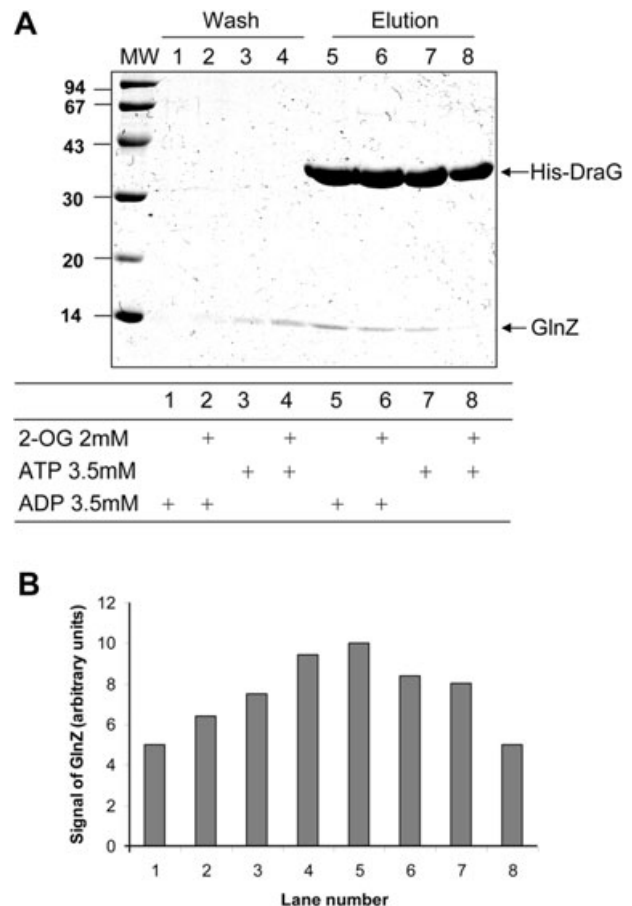


Fig. 5. The presence of either 2-OG or ATP can partially dissociate the DraG-GlnZ complex. (A) The HisDraG-GlnZ complex was immobilized on Ni²⁺ beads in binding buffer (Fig. 4) plus 3.5 mM ADP. Beads were washed (Wash) with buffer containing ADP or ATP and 2-OG as indicated in the Table. Bound proteins were eluted with 0.5 M imidazole (Elution). The samples were submitted to SDS-PAGE, the gel was stained with Coomassie blue and the signal for GlnZ was quantified by densitometry (B). Arrows indicate the identified proteins.

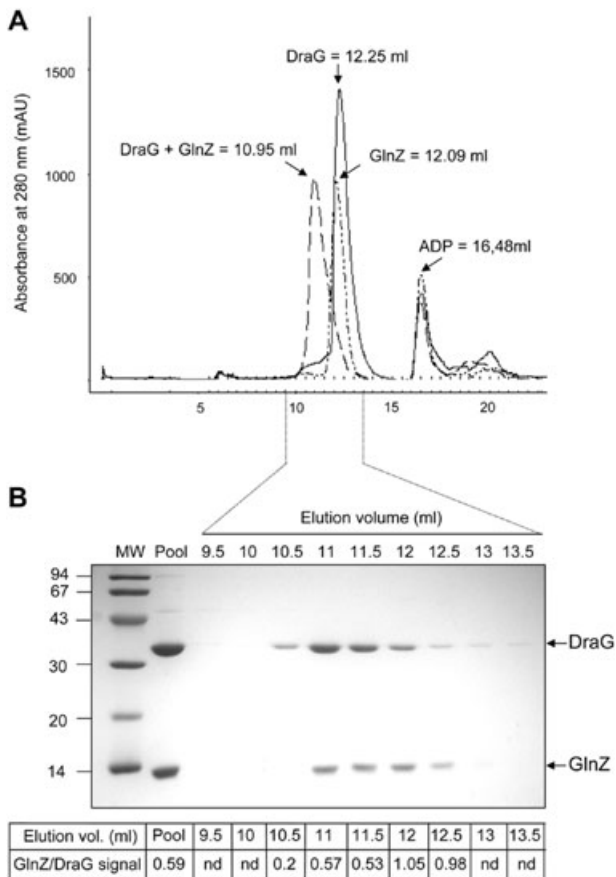


Fig. 6. Gel filtration analysis of the DraG–GlnZ complex. Gel filtration was performed on a Superose 12 10/30 GL column using 50 mM Tris-HCl, pH 8.0, 10% (v/v) glycerol, 0.05% (w/v) LDAO, 100 mM NaCl, 1 mM MgCl₂, 1 mM ADP as buffer. Runs were performed at room temperature at a flow rate of 0.5 ml min⁻¹, the column was calibrated with a range of molecular mass standards (Sigma). Purified proteins (DraG and/or GlnZ) were incubated in 50 mM Tris-HCl, pH 8.0, 10% (v/v) glycerol, 0.05% (w/v) LDAO, 100 mM NaCl, 1 mM MgCl₂, 5 mM MnCl₂ and 3.5 mM ADP for 20 min on ice before loading.
 A. The graphic shows the elution volume from each sample, DraG alone = 12.25 ml, GlnZ alone = 12.09 ml and DraG plus GlnZ = 10.95 ml. In all runs, including a control without protein, we observed a peak of ADP at 16.48 ml as it was loaded in higher concentration than in the running buffer.
 B. When DraG plus GlnZ were loaded, samples were collected every 500 µl and 10 µl were analysed in 12.5% SDS-PAGE gels, the gel was stained with Coomassie blue. Arrows indicate the identified proteins and (Pool) indicates a fraction of the loaded sample. The table below shows the ratio of the GlnZ to DraG signal in the gel reported as arbitrary units. nd, not determined.

native DraG (data not shown). Two reasons can account for this apparent discrepancy. First, as the GlnZ–DraG interaction is transient and the dissociation constant not known it is possible that some GlnZ is lost owing to complex dissociation during the wash steps. Second, the His-DraG is immobilized onto the solid matrix, a situation where its binding surface may be less accessible or unavailable to GlnZ. In the gel filtration assays the DraG–

GlnZ complex is separated from the DraG monomer (34 kDa) and GlnZ trimer (38 kDa), and the relative abundance of each protein in the fraction corresponding to the molecular mass of the complex reflects its stoichiometry. A similar effect has been recently reported for the Atase–GlnB complex in *E. coli* (Jiang *et al.* 2007) where different complex stoichiometries were observed depending on the technique used.

In vitro formation of the HisAmtB–GlnZ–DraG ternary complex

Having established conditions for the formation of AmtB–GlnZ and GlnZ–DraG complexes, we investigated the formation of the putative ternary complex between AmtB, GlnZ and DraG. Using Ni²⁺ beads, native DraG was assayed for coprecipitation together with HisAmtB and either GlnZ or GlnB. Figure 7 shows the result of ternary complex formation in the presence ADP and MnCl₂. As controls we used all protein combinations in the absence of HisAmtB, i.e. DraG alone, DraG plus GlnZ and DraG

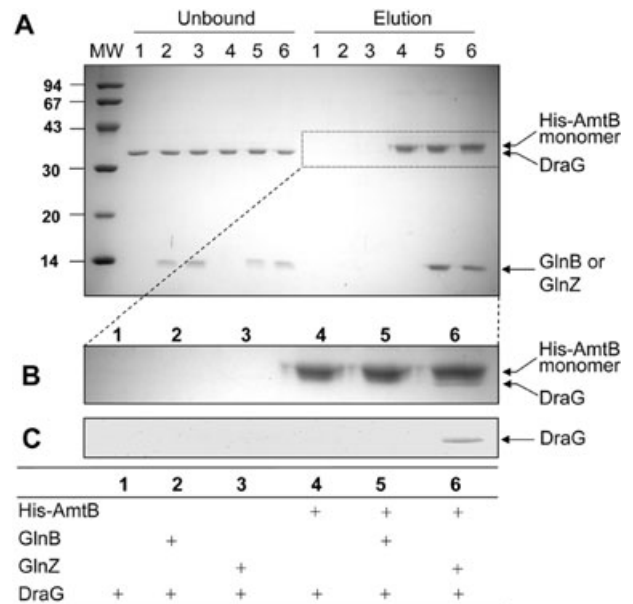


Fig. 7. *In vitro* formation of the AmtB–GlnZ–DraG ternary complex. Complex formation was assayed by coprecipitation using Ni²⁺ beads. The reactions were conducted in buffer containing 50 mM Tris-HCl pH 8.0, 0.1 M NaCl, 0.05% LDAO, 10% glycerol, 20 mM imidazole, 3.5 mM ADP, 1 mM MgCl₂ and 5 mM MnCl₂. Binding reactions were performed in 500 µl of buffer adding the purified proteins at the following concentrations: 0.15 µM HisAmtB and 0.5 µM GlnZ or GlnB and 1 µM DraG. Beads were washed and bound proteins were eluted with 0.5 M imidazole (Elution).
 A. The unbound (supernatant of the binding reaction) and eluted fractions were analysed by SDS-PAGE and the gel was stained with Coomassie blue. The arrows indicate the identified proteins.
 B. Magnification of the eluted fractions in the Coomassie blue stained gel.
 C. Magnification of the eluted fractions subjected to Western blotting using an anti-DraG antibody.

plus GlnB. None of these combinations showed any binding (Fig. 7B, lanes 1, 2 and 3).

In the presence of HisAmtB, DraG was not present in the elution (Fig. 7B, lane 4) indicating that AmtB is not capable of interacting with DraG directly. In the reaction containing HisAmtB plus GlnB and DraG, we observed only HisAmtB and GlnB in the elution (Fig. 7A, lane 5). Hence, while formation of the AmtB–GlnB binary complex occurs under these conditions, this complex is not capable of interacting with DraG (Fig. 7B, lane 5).

In the reaction containing HisAmtB plus GlnZ and DraG, we observed all three proteins HisAmtB, GlnZ and DraG in the elution (Fig. 7B, lane 6). The band assigned as DraG in Fig. 7B, lane 6 was confirmed to be DraG by Western blot with anti-DraG antibody (Fig. 7C) and also by MALDI-TOF mass spectrometry analysis where two peaks with a *m/z* of 1773.217 and 1940.250 were identified which match two predicted *A. brasilense* DraG peptides (*m/z* 1772.918, from amino acid residue 132 to 148 and 1939.954, from 53 to 70, giving a protein coverage of 11.8%).

These results demonstrate that DraG can interact with the AmtB–GlnZ complex but not with the AmtB–GlnB complex, confirming our *in vitro* P_{II}–DraG interaction data and in agreement with our previous *in vivo* observations (Huergo *et al.*, 2006b). Ternary complex formation was not observed when ADP was substituted by ATP in the binding buffer (data not shown). This probably reflects the requirement of ADP for the stabilization of the DraG–GlnZ complex (Fig. 4). We also tested the capacity of ATP or ATP plus 2-OG to dissociate the AmtB–GlnZ–DraG ternary complex and we found that while ATP alone had no effect, in the presence of ATP plus 2 mM 2-OG the ternary complex was completely dissociated (data not shown). This effect is probably related to the instability of the AmtB–GlnZ interaction under these conditions (Fig. 1A and 3).

Discussion

In this study we have used an *in vitro* reconstitution system with purified proteins to validate successfully our previous model developed from our *in vivo* studies. Consequently, we have confirmed that under appropriate conditions the nitrogenase regulatory enzyme DraG is sequestered to the cell membrane by formation of an AmtB–GlnZ–DraG ternary complex. We have also established the *in vitro* conditions to obtain the AmtB–GlnZ and GlnZ–DraG binary complexes and we have evaluated the effects of the P_{II} effector molecules on the stability of all of these complexes.

AmtB–P_{II} interaction

First, we studied *in vitro* interactions between the *A. brasilense* ammonia channel AmtB and the P_{II} proteins,

GlnB and GlnZ. This is the third report showing *in vitro* interaction between purified members of the Amt and P_{II} protein families; the other studies were conducted using AmtB and GlnK proteins from *E. coli* (Durand and Merrick, 2006) and from the archaeon *Methanococcus jannaschii* (Yildiz *et al.*, 2007). Both previous studies showed inhibition of complex formation in the presence of Mg-ATP and 2-OG. A recent report in *R. rubrum* has shown that the P_{II} protein GlnJ can interact with AmtB1-containing membranes, this interaction is disrupted in the presence of ATP plus 2-OG (Wolfe *et al.*, 2007). Our results with the *A. brasilense* AmtB–P_{II} complexes shows a similar response (Fig. 1), even very low concentrations of 2-OG are inhibitory, e.g. 10 μM which is far below the physiological levels reported for *E. coli* (from 0.1 to 0.9 mM accordingly to Senior, 1975) when used in combination with Mg-ATP. Interestingly, both in *E. coli* (Durand and Merrick, 2006) and in *A. brasilense* (Fig. 1), the inhibition caused by 2-OG on the AmtB–P_{II} complex formation is only observed in the presence of Mg²⁺. Two possible hypotheses can be suggested to explain the role of Mg²⁺. As the ATP and 2-OG binding sites are probably close to each other in the P_{II} proteins as previously proposed (Benelli *et al.*, 2002; Durand and Merrick, 2006), a positively charged Mg²⁺ ion may be necessary to stabilize the binding of the two negatively charged molecules, 2-OG and ATP. Hence, simultaneous binding of 2-OG and ATP to P_{II} can only occur in the presence of Mg²⁺ (Durand and Merrick, 2006). Alternatively, based on crystallographic structures of *M. jannaschii* GlnK1, it was proposed that the binding site for 2-OG is only created when Mg-ATP is bound to GlnK1, in which case the presence of ATP alone would not be sufficient to generate the 2-OG binding site (Yildiz *et al.*, 2007).

Recently, the crystal structures of the AmtB–GlnK complex of *E. coli* formed both *in vivo* (Conroy *et al.*, 2007) and *in vitro* (Gruswitz *et al.*, 2007) were determined. In both cases, the GlnK protein was found in an ADP-bound state, even though crystallization of the *in vitro*-formed complex was conducted in the presence of ATP. Bonds between main chain NH groups of GlnK and phosphate oxygen atoms of ADP induce a tight turn in the GlnK structure and potentially help to position the GlnK T-loop into the cytoplasmic vestibule of the AmtB protein (Conroy *et al.*, 2007; Gruswitz *et al.*, 2007). The *in vitro* effects of ADP or AMP were not reported for *E. coli* AmtB–GlnK complex formation (Durand and Merrick, 2006). However, for *A. brasilense* we observed interaction between AmtB–P_{II} in the presence of ATP, ADP or AMP (Figs 1 and 2A), suggesting that any of these adenosine nucleotides may potentially induce such a turn and allow complex formation.

Although both ATP and ADP induce AmtB–GlnZ complex formation, these complexes show different responses to

2-OG. Whereas 2-OG promotes dissociation of the complex in the presence of ATP and $MgCl_2$ no such effect is observed when ATP is substituted by ADP (Fig. 3). A similar response was reported with the GlnJ–AmtB1 pair from *R. rubrum* (Wolfe *et al.*, 2007). ATP and 2-OG have been reported to bind the *E. coli* GlnB protein synergistically (Jiang *et al.*, 1998), but the same synergy has not been observed for ADP and 2-OG (Kamberov *et al.*, 1995; Ruppert *et al.*, 2002; Maheswaran *et al.*, 2004). Hence, one explanation for the observed difference between the effects of 2-OG in the presence of ATP or ADP could be that Mg^{2+} facilitates the synergistic binding of ATP and 2-OG but this cannot occur when ADP replaces ATP. Consequently, 2-OG only binds to GlnZ in the presence of ATP and $MgCl_2$, whereupon it brings about a GlnZ T-loop conformation that is not compatible with AmtB binding and the complex dissociates. Alternatively, both ATP- and ADP-bound forms of GlnZ could bind 2-OG equivalently but show different conformations in the T-loop.

Taken together, our data strongly suggest that in *A. brasilense* only the ADP-bound complex is stable under physiologically relevant conditions (i.e. in the presence of Mg^{2+}) and this complex would be relatively insensitive to changes in the 2-OG pool. By contrast the ATP-bound complex is sensitive to 2-OG levels (Fig. 3). Hence, the cellular ATP:ADP ratio and 2-OG levels appear to play major and minor roles, respectively, in complex stability such that a sufficient ATP pool would be a prerequisite for 2-OG-mediated dissociation of the complex.

GlnZ–DraG interaction and AmtB–GlnZ–DraG ternary complex formation

Our previous work has indicated that in *A. brasilense* the nitrogenase regulatory enzyme DraG can form a complex with GlnZ *in vivo* independently of the GlnZ uridylylation status (Huergo *et al.*, 2006b). Here we show, for the first time, the *in vitro* reconstitution of a complex of de-uridylylated GlnZ with DraG. We observe very faint GlnZ–DraG interaction in the absence of nucleotides. The formation of the complex is positively influenced by ADP (Fig. 4). It is possible that the weak interaction observed in the absence of ADP might be the result of ADP carried over by GlnZ during purification. A recent report has shown a similar effect for the GlnK1 from *M. jannaschii* (Yildiz *et al.*, 2007). We observed slightly different results for the HisDraG–GlnZ complex in the absence of nucleotides using different GlnZ preparations (data not shown).

The DraG–GlnZ complex can be partially dissociated by adding either 2-OG or ATP alone: a combination of these two effectors leads to stronger dissociation (Fig. 5). We believe that the ADP and 2-OG effects are likely to be mediated via the known interaction of P_{II} proteins (in this case GlnZ) with these effectors, although we cannot

formally exclude an interaction of ADP and/or 2-OG with DraG. Gel filtration analysis revealed a 1:1 DraG monomer : GlnZ trimer stoichiometry for the complex formed in presence of ADP (Fig. 6).

Previously we observed that *in vivo* GlnZ–DraG complex formation is independent of the cellular nitrogen levels, though a stronger interaction was observed after an ammonium shock (Huergo *et al.*, 2006b). The physiological relevance of the positive influence of ADP for *in vitro* GlnZ–DraG complex formation is still unclear; it may be possible that ADP increases the affinity of GlnZ for DraG after an ammonium shock (see Discussion later). To our knowledge, the *A. brasilense* AmtB– P_{II} and GlnZ–DraG complexes studied here are only the second and third examples showing the effects of ADP and ATP on complex formation by a P_{II} protein. The other study was with the P_{II} –NAGK complex from *Synechococcus elongatus* (Maheswaran *et al.*, 2004), where an inhibitory effect of ADP on complex formation was observed. The other study was with the P_{II} –NAGK complex from *Synechococcus elongatus* (Maheswaran *et al.*, 2004), where an inhibitory effect of ADP on complex formation was observed. Recently Wolfe *et al.* (2007) also showed that ADP affected binding of GlnJ from *Rhodobacter capsulatus* to AmtB1-containing membrane fraction. In all these cases, different effects on the complex stability were observed whether ADP or ATP was present, offering new insights into the energy-sensing properties of P_{II} proteins. In all these cases, different effects on the complex stability were observed whether ADP or ATP was present, offering new insights into the energy-sensing properties of P_{II} proteins.

Having established the conditions to form both AmtB–GlnZ and GlnZ–DraG complexes *in vitro* we were able to reconstitute a ternary complex involving all three proteins (Fig. 7). This result confirmed previous *in vivo* data which suggested the formation of such a complex in *A. brasilense* (Huergo *et al.*, 2006a,b) and in *R. rubrum* (Wang *et al.*, 2005; Zhang *et al.*, 2006).

An overview of the events following ammonium shock in A. brasilense and the putative physiological relevance of the P_{II} effectors on the AmtB– P_{II} complex formation

In vivo data from both *E. coli* and *A. brasilense* have shown that the AmtB– P_{II} complex formation only occurs after an ammonium shock, when P_{II} proteins are de-uridylylated (Coutts *et al.*, 2002; Javelle *et al.*, 2004; Huergo *et al.*, 2006a). The addition of ammonium to nitrogen-limited *E. coli* cells has been shown to cause a 10-fold drop in the intracellular ATP levels within 15 s (Schutt and Holzer, 1972). We speculate that the ammonium added to nitrogen-limited cells is rapidly assimilated by glutamine synthetase leading to an increase in the glutamine levels and a drop in the ATP and 2-OG levels.

High glutamine triggers GlnD uridylyl-removing activity leading to P_{II} protein de-uridylylation which, together with a decrease in the ATP : ADP ratio and 2-OG levels, favours AmtB– P_{II} complex formation and channel inactivation. Simultaneously, increased ADP levels would stimulate the interaction between de-uridylylated GlnZ and DraG and allow ternary complex formation, targeting DraG to the cell membrane and effectively inactivating the enzyme, either by sequestration away from its substrate or by conformational change. Once the added ammonium is exhausted by cellular metabolism, the ATP and 2-OG levels will rise allowing GlnZ to dissociate from AmtB, thus liberating DraG to interact with its cytosolic substrate, the ADP-ribosylated NifH. As judged by the structural data on the *E. coli* AmtB–GlnK complex (Conroy *et al.*, 2007; Gruswitz *et al.*, 2007), the observed role of ATP and 2-OG in disrupting the AmtB– P_{II} complex (Fig. 3) may be a steric prerequisite for the accession of GlnD to the P_{II} T-loop, allowing P_{II} re-uridylylation once the glutamine levels drop.

Membrane sequestration of P_{II} targets as a potentially widespread regulatory mechanism

When complex formation between *E. coli* AmtB and GlnK was first demonstrated, it was suggested that complex formation might not only regulate AmtB channel activity but could also play a role in affecting P_{II} interaction with other P_{II} targets, by reducing the P_{II} protein levels in the cytosol (Coutts *et al.*, 2002). Recent studies have indicated that the AmtB– P_{II} complex might sequester other P_{II} targets to the cell membrane, and that this could provide a regulatory mechanism.

In addition to sequestration of DraG in either *A. brasilense* (Huergo *et al.*, 2006a,b) or *R. rubrum* (Wang *et al.*, 2005), another potentially similar regulatory situation has recently been described in *Bacillus subtilis*. In this case it was shown that the *B. subtilis* master regulator of nitrogen metabolism, TnrA, is targeted to the cell membrane under certain conditions in a GlnK and AmtB-dependent manner, and it was therefore proposed that membrane sequestration may regulate TnrA activity (Heinrich *et al.*, 2006).

In this study we have shown for the first time that a ternary complex involving AmtB– P_{II} and a P_{II} target, in this case DraG, can indeed occur. As P_{II} proteins have a long list of known targets in a wide range of organisms, it seems likely that ternary complex formation involving AmtB and P_{II} could be a wide-spread regulatory mechanism in prokaryotes. The control of regulatory or catalytic proteins of nitrogen metabolism by AmtB– P_{II} -dependent membrane sequestration would provide an excellent regulatory switch, responding not only to the nitrogen levels, via the P_{II} modification status, but also to the

energy and carbon levels as ATP, ADP and 2-OG regulate the AmtB– P_{II} interaction.

Experimental procedures

Plasmid construction

Plasmid pLHPETHisAmtB encodes an N-terminally 6His-tagged version of *A. brasilense* AmtB in which the 6His tag was inserted three residues downstream of the predicted signal peptide cleavage sequence. The 6His insertion was obtained by overlap PCR using genomic DNA from *A. brasilense* strain FP2 (Pedrosa and Yates, 1984) as template. The 5' end of *amtB* (120 bp) was PCR-amplified with the primers AmtB-NT 5'-AGCCTCCATGGGCCGTCTCTTCACCCTCGC-3' (NcoI restriction site underlined) and AmtB-HisR 5'-GCGTGGTGGTGGTGGTGGTGGCTTTCC TGGGCGAGGGCGG-3'. The 3' end of *amtB* (1.3kb) was PCR-amplified with the primers AmtB-HisF 5'-GCCA CCACCACCACCACGCGCCGCCGCGGCCGAACC-3' and AmtB-CT 5'-ATGGAGAATTC AACCAGGCAGCAAGG GTGC-3' (EcoRI restriction site underlined). The PCR products were gel extracted, annealed and used as template in a third PCR reaction with primers AmtB-NT and AmtB-CT. The PCR product was digested with NcoI and EcoRI and ligated to the pETBlue vector, previously digested with the same enzymes, to yield plasmid pLHPblueHisAmtB. The NcoI–EcoRI fragment from pLHPblueHisAmtB was transferred to the pET28a vector digested with the same enzymes to give pLHPETHisAmtB. The DNA insert of pLHPETHisAmtB was fully sequenced to check its integrity.

In order to express the *his-amtB* allele in *A. brasilense* we used our previously described strategy (Huergo *et al.*, 2005b). The XbaI–HindIII fragment from the pLHPETHisAmtB plasmid was subcloned into the pDK7 vector, generating pLHDK7HisAmtB. This plasmid was co-integrated with the pMP220 vector generating pLHMPHisAmtB which expresses the *his-amtB* gene from the *ptac* promoter under the control of LacI. The pLHMPHisAmtB plasmid was inserted into the *A. brasilense* FAJ310 (*amtB:km*) strain by conjugation as described (Huergo *et al.*, 2005b).

The pLHPETDraGwt plasmid, which encodes wild type *A. brasilense* DraG, was obtained as follows. The *draG* gene (900 bp) was PCR-amplified using genomic DNA of *A. brasilense* strain FP2 as template and the primers DraG5Nco 5'-CCGGCCCATGGCTGACCATTCCATCC-3' (NcoI restriction site underline) and DraG3' (Huergo *et al.*, 2005a). The PCR product was digested with NcoI and EcoRI and ligated to the pET28a vector previously digested with the same enzymes to give plasmid pLHPETDraGwt. The DNA insert of pLHPETDraGwt was fully sequenced to check its integrity.

The pLMA-MLV1 plasmid, which encodes an N-terminally 6His-tagged version of *A. brasilense* GlnB, was obtained as follows. The *glnB* gene (300 bp) was PCR-amplified using genomic DNA of *A. brasilense* strain FP2 as template and the primers AbglnB5': 5'-CTCGTACCCATGGGACATATGAAGA AGATCGAA-3' (NdeI restriction site underline) and AbglnB3': 5'-TATATAGGATCCTCAGAGAGCTTCGGT-3' (BamHI restriction site underline). The PCR product was digested with NdeI and BamHI and ligated to the pET28a vector previously digested with the same enzymes to give plasmid pLMA-

MLV1. The DNA insert of pLMA-MLV1 was fully sequenced to check its integrity.

Protein analysis

Electrophoresis of proteins was carried out by SDS-PAGE and gels were Coomassie blue stained. Signals on SDS-PAGE stained gels were quantified using the Laboratory Works program (UVP); the results are reported in arbitrary units. Protein concentrations were determined by the Bradford assay using bovine serum albumin as standard. Western blots were carried out as described (Huergo *et al.*, 2006a), using monoclonal mouse anti-His antibody (GE-Healthcare) or polyclonal rabbit anti-DraG or anti-NifH antibody (Huergo *et al.*, 2005a). The ADP-ribosylation of NifH in *A. brasilense* was monitored as described (Huergo *et al.*, 2006a).

For MALDI-TOF analysis protein bands were excised from gels, de-stained with 50% (v/v) acetonitrile containing 25 mM NH_4HCO_3 , dehydrated in 50 μl of acetonitrile for 10 min and dried under vacuum for 25 min. Samples were treated with 10 μl of 25 mM NH_4HCO_3 containing 0.2 μg of porcine trypsin (Promega) overnight at 37°C. The supernatant was dried under vacuum and peptides were reconstituted in 0.1% (v/v) trifluoroacetic acid. The sample was mixed with α -cyano-4-hydroxycinnamic acid matrix (1:1), spotted on a Maldi plate (Bruker Daltonics) and allowed to dry. The dried sample was analysed using a MALDI-TOF-MS Auto-flex spectrometer (Bruker Daltonics).

HisAmtB purification

Six litres of *E. coli* C43 cells carrying pLHPETHisAmtB was grown in Luria-Bertani (LB) medium supplemented with NH_4Cl 40 mM at 37°C to an OD_{600} of 0.5. To induce HisAmtB expression, IPTG 0.3 mM was added and, after for 4 h, cells were harvested by centrifugation. The pellet was resuspended in 60 ml of 50 mM Tris-HCl pH 8, 0.1 M NaCl, 10% glycerol and lysed by two passages through a French pressure cell, 15000 psi at 4°C. The extract was clarified by centrifugation at 30 000 *g* for 30 min at 4°C. The supernatant (whole-cell extract) was centrifuged at 200 000 *g* for 1 h at 4°C. The membrane pellet was resuspended in 10 ml of 50 mM Tris-HCl pH 8, 0.1 M NaCl, 10% glycerol, 2% LDAO (n-dodecyl-N,N-dimethylamine-N-oxide) and mixed gently for 1 h on ice. After another centrifugation step (200 000 *g* for 1 h at 4°C), the supernatant was applied to a 1 ml Hi-Trap chelating column prepared by saturating with 100 mM NiCl_2 , and equilibrated with buffer 1 (50 mM Tris-HCl pH 8, 0.6 M NaCl, 10% glycerol, 0.05% LDAO) at 1 ml min^{-1} . The column was washed with 10 ml of buffer 1 and 5 ml of buffer 2 (50 mM Tris-HCl pH 8, 0.1 M NaCl, 10% glycerol, 0.05% LDAO, 10 mM imidazole). Protein was eluted in buffer 2 containing 50, 100, 300 or 500 mM imidazole in 5 ml steps. Fractions containing HisAmtB (peak at 300 mM imidazole) were pooled and dialysed in 50 mM Tris-HCl pH 8, 0.1 M NaCl, 50% glycerol, 0.05% LDAO. HisAmtB was more than 92% pure as judged by densitometric analysis of a Coomassie-stained gel.

Purification of GlnB, GlnZ, HisGlnB and HisGlnZ

For purification of native P_{II} proteins from *A. brasilense*, one litre of *E. coli* BL21 (DE3) cells carrying pLH25PET

(expressing GlnB) (Huergo *et al.*, 2005b) or pMSA4 (expressing GlnZ) (Araujo *et al.*, 2004) was grown in LB medium supplemented with NH_4Cl 40 mM at 37°C to an OD_{600} of 0.5. IPTG (0.3 mM) was added and, after for 4 h, cells were harvested by centrifugation. The pellet was resuspended in 30 ml of 50 mM Tris-HCl pH 7.5, 0.1 M KCl, 1 mM EDTA, 20% glycerol. Cells were disrupted by sonication, cell extract was clarified by centrifugation (30 000 *g* for 30 min at 4°C). The supernatant was loaded onto a 5 ml Hi-Trap Heparin column (GE-Healthcare) previously equilibrated with buffer A (50 mM Tris-HCl pH 7.5, 0.1 M KCl, 1 mM EDTA). Protein was eluted with a linear gradient up to 1.1 M KCl in buffer A. Fractions containing GlnB or GlnZ, which peaked at 0.4 M KCl, were collected and dialysed in 50 mM Tris-HCl pH 7.5, 0.1 M KCl, 20% glycerol. GlnB and GlnZ were more than 90% pure as judged by densitometric analysis of a Coomassie-stained gel. The homogeneity of the preparations were also confirmed by native gel and MALDI-TOF analysis.

For the purification of N-terminal 6His-tagged P_{II} proteins from *A. brasilense*, the HisGlnB and HisGlnZ proteins were overexpressed in *E. coli* BL21 (DE3) cells carrying pLMA-MLV1, expressing HisGlnB, or pMSA3, expressing HisGlnZ (Araujo *et al.*, 2004). Protein purification was conducted as described (Araujo *et al.*, 2004) with the following modifications: protamine sulphate precipitation was excluded and DTT was not included in buffers.

DraG purification

For the purification of native *A. brasilense* DraG, one litre of *E. coli* BL21 (DE3) cells carrying pLHPETDraGwt was grown in LB medium supplemented with NH_4Cl 40 mM at 37°C to an OD_{600} of 0.5. IPTG 0.3 mM was added and cells were incubated for 20 h at 20°C. Cells were harvested by centrifugation and resuspended in 30 ml of 50 mM Tris-HCl pH 8, 0.1 M NaCl, 10% glycerol, 0.5 mM MnCl_2 . Cells were disrupted by sonication and the cell extract was clarified by centrifugation (30 000 *g* for 30 min at 4°C). The supernatant was loaded onto a 5 ml Hi-Trap Heparin column (GE-Healthcare) previously equilibrated with buffer A (50 mM Tris-HCl pH 8, 0.1 M NaCl). Protein was eluted with a linear gradient of buffer A, up to 1.1 M NaCl. Fractions containing DraG, which peaked at 0.4 M NaCl, were collected and dialysed in 50 mM Tris-HCl pH 8, 0.1 M NaCl, 50% glycerol, 0.5 mM MnCl_2 . DraG was 99% pure as judged by densitometric analysis of a Coomassie-stained gel.

For the purification of N-terminal 6His-tagged *A. brasilense* DraG, induction was performed in *E. coli* BL21 (DE3) cells carrying pLHPETDraG (Huergo *et al.*, 2005a) and the cell extract prepared essentially as described for native DraG. After cell extract clarification, the supernatant was applied to a 1 ml Hi-Trap chelating column, followed by elution and dialysis essentially as described for HisAmtB except that LDAO was not included in buffers. HisDraG precipitated after elution and dialysis. Precipitated samples were subjected to centrifugation at 30 000 *g* for 10 min at 4°C and only the supernatant was used for further analysis. HisDraG was more than 99% pure as judged by densitometric analysis of a Coomassie-stained gel.

In vitro complex formation

In vitro complex formation was assayed using HisMagnetic beads according to the manufacturer's instructions (Promega). All reactions were conducted in buffer containing 50 mM Tris-HCl pH 8, 0.1 M NaCl, 0.05% LDAO, 10% glycerol, 20 mM imidazole in the presence or absence of effectors (MgCl₂, MnCl₂, 2-OG, ATP, ADP, AMP) as indicated in each experiment. Twenty-five microlitres of beads was equilibrated by two washes with 200 µl of buffer. Binding reactions were performed in 500 µl of buffer by adding purified proteins: 0.15 µM HisAmtB, 0.5 µM GlnB or GlnZ, HisGlnB or HisGlnZ, 1 µM DraG in this order. Protein concentrations were calculated assuming HisAmtB, GlnB and GlnZ to be trimers and DraG to be a monomer. After 5 min, the beads were washed three times with 300 µl of buffer. Elution was performed incubating the beads with 50 µl of buffer containing 0.5 M imidazole for 5 min. Eluted samples were mixed with sample buffer and analysed in 12.5% SDS-PAGE stained with Coomassie blue. For complex dissociation assays, the beads were washed with 50 µl of buffer containing the effectors prior to elution with imidazole.

Gel filtration analysis of the DraG–GlnZ complex

Gel filtration chromatography was performed on a Superose 12 10/30 GL column using 50 mM Tris-HCl, pH 8.0, 10% (v/v) glycerol, 0.05% (w/v) LDAO, 100 mM NaCl, 1 mM MgCl₂, 1 mM ADP as buffer. The elution volumes indicated are an average of two independent runs. The Superose 12 HR 10/30 was calibrated with following molecular mass markers (Sigma; their elution volumes are in parentheses): α-amylase, 200 kDa (9.49 ml); alcohol deshydrogenase, 150 kDa (10.13 ml); bovine serum albumin, 66 kDa (10.72 ml); carbonic anhydrase, 29 kDa (12.55 ml); cytochrome c, 12.4 kDa (14.13 ml). Purified proteins (DraG and/or GlnZ) were incubated in 50 mM Tris-HCl, pH 8.0, 20% (v/v) glycerol, 100 mM NaCl, 1 mM MgCl₂, 5 mM MnCl₂ and 3.5 mM ADP for 20 min on ice before loading. The loaded samples consisted of GlnZ (18 µmol as trimer), DraG (18 µmol as monomer) or DraG plus GlnZ (18 µmol each) in 200 µl. Runs were performed at room temperature at a flow rate of 0.5 ml min⁻¹, and 10 µl of the collected fractions (500 µl) was analysed in 12.5% SDS-PAGE gels.

Acknowledgements

We are grateful to Daniela F. Seixas for helping with the MALDI-TOF analysis. Valter de Baura, Roseli Prado and Julieta Pie are thanked for their technical support. This work was supported by CNPq (Instituto do Milênio) and Fundação Araucária. L.F.H. is supported by a PDJ fellowship from the CNPq-Brazil. M.J.M. acknowledges support from the Biotechnology and Biological Sciences Research Council (UK).

Note added in proof

Jiang and Ninfa reported recently (Biochemistry, doi: 10.1021/bi701062t) that ADP affects *E. coli* P_{II} regulation of ATase and NtrB, and also the uridylylation of P_{II} by GlnD.

References

- Andrade, S.L., Dickmanns, A., Ficner, R., and Einsle, O. (2005a) Crystal structure of the archaeal ammonium transporter Amt-1 from *Archaeoglobus fulgidus*. *Proc Natl Acad Sci USA* **102**: 14994–14999.
- Andrade, S.L., Dickmanns, A., Ficner, R., and Einsle, O. (2005b) Expression, purification and crystallization of the ammonium transporter Amt-1 from *Archaeoglobus fulgidus*. *Acta Crystallogr* **61**: 861–863.
- Araujo, M.S., Baura, V.A., Souza, E.M., Benelli, E.M., Rigo, L.U., Steffens, M.B., *et al.* (2004) *In vitro* uridylylation of the *Azospirillum brasilense* N-signal transducing GlnZ protein. *Protein Expr Purif* **33**: 19–24.
- Arcondéguy, T., Jack, R., and Merrick, M. (2001) P_{II} signal transduction proteins: pivotal players in microbial nitrogen control. *Microbiol Mol Biol Rev* **65**: 80–105.
- Benelli, E.M., Buck, M., Polikarpov, I., de Souza, E.M., Cruz, L.M., and Pedrosa, F.O. (2002) *Herbaspirillum seropedicae* signal transduction protein P_{II} is structurally similar to the enteric GlnK. *Eur J Biochem* **269**: 3296–3303.
- Blakey, D., Leech, A., Thomas, G.H., Coutts, G., Findlay, K., and Merrick, M. (2002) Purification of the *Escherichia coli* ammonium transporter AmtB reveals a trimeric stoichiometry. *Biochem J* **364**: 527–535.
- Conroy, M.J., Durand, A., Lupo, D., Li, X.D., Bullough, P.A., Winkler, F.K., and Merrick, M. (2007) The crystal structure of the *Escherichia coli* AmtB–GlnK complex reveals how GlnK regulates the ammonia channel. *Proc Natl Acad Sci USA* **104**: 1213–1218.
- Coutts, G., Thomas, G., Blakey, D., and Merrick, M. (2002) Membrane sequestration of the signal transduction protein GlnK by the ammonium transporter AmtB. *EMBO J* **21**: 1–10.
- Detsch, C., and Stulke, J. (2003) Ammonium utilization in *Bacillus subtilis*: transport and regulatory functions of NrgA and NrgB. *Microbiol* **149**: 3289–3297.
- Durand, A., and Merrick, M. (2006) *In vitro* analysis of the *Escherichia coli* AmtB–GlnK complex reveals a stoichiometric interaction and sensitivity to ATP and 2-oxoglutarate. *J Biol Chem* **281**: 29558–29567.
- Forchhammer, K. (2004) Global nitrogen/carbon control by P_{II} signal transduction in cyanobacteria: from signals to targets. *FEMS Microbiol Rev* **28**: 319–333.
- Forchhammer, K., and Hedler, A. (1997) Phosphoprotein P_{II} from cyanobacteria: analysis of functional conservation with the P_{II} signal protein from *Escherichia coli*. *Eur J Biochem* **244**: 869–875.
- Gruswitz, F., O'Connell, J. III and Stroud, R.M. (2007) Inhibitory complex of the transmembrane ammonia channel, AmtB, and the cytosolic regulatory protein, GlnK, at 1.96 Å. *Proc Natl Acad Sci USA* **104**: 42–47.
- Heinrich, A., Woyda, K., Brauburger, K., Meiss, G., Detsch, C., Stulke, J., and Forchhammer, K. (2006) Interaction of the membrane-bound GlnK–AmtB complex with the master regulator of nitrogen metabolism TnrA in *Bacillus subtilis*. *J Biol Chem* **281**: 34909–34917.
- Huergo, L.F., Souza, E.M., Steffens, M.B., Ates, M.G., Pedrosa, F.O., and Chubatsu, L.S. (2005a) Effects of over-expression of the regulatory enzymes DraT and DraG on the ammonium-dependent post-translational regulation of

- nitrogenase reductase in *Azospirillum brasilense*. *Arch Microbiol* **183**: 209–217.
- Huergo, L.F., Filipaki, A., Chubatsu, L.S., Yates, M.G., Steffens, M.B., Pedrosa, F.O., and Souza, E.M. (2005b) Effect of the over-expression of PII and PZ proteins on the nitrogenase activity of *Azospirillum brasilense*. *FEMS Microbiol Lett* **253**: 47–54.
- Huergo, L.F., Souza, E.M., Araujo, M.S., Pedrosa, F.O., Chubatsu, L.S., Steffens, M.B., and Merrick, M. (2006a) ADP-ribosylation of dinitrogenase reductase in *Azospirillum brasilense* is regulated by AmtB-dependent membrane sequestration of DraG. *Mol Microbiol* **59**: 326–337.
- Huergo, L.F., Chubatsu, L.S., Souza, E.M., Pedrosa, F.O., Steffens, M.B., and Merrick, M. (2006b) Interactions between PII proteins and the nitrogenase regulatory enzymes DraT and DraG in *Azospirillum brasilense*. *FEBS Lett* **580**: 5232–5236.
- Javelle, A., Severi, E., Thornton, J., and Merrick, M. (2004) Ammonium sensing in *Escherichia coli*. Role of the ammonium transporter AmtB and AmtB-GlnK complex formation. *J Biol Chem* **279**: 8530–8538.
- Jiang, P., Peliska, J.A., and Ninfa, A.J. (1998) Enzymological characterization of the signal-transducing uridylyltransferase/uridylyl-removing enzyme (EC 2.7.7.59) of *Escherichia coli* and its interaction with the PII protein. *Biochemistry* **37**: 12782–12794.
- Jiang, P., Pioszak, A.A., and Ninfa, A.J. (2007) Structure-function analysis of glutamine synthetase adenylyltransferase (ATase, EC 2.7.7.49) of *Escherichia coli*. *Biochemistry* **46**: 4117–4132.
- Kamberov, E.S., Atkinson, M.R., and Ninfa, A.J. (1995) The *Escherichia coli* PII signal transduction protein is activated upon binding 2-ketoglutarate and ATP. *J Biol Chem* **270**: 17797–17807.
- Khademi, S., O'Connell, J. III, Remis, J., Robles-Colmenares, Y., Miercke, L.J., and Stroud, R.M. (2004) Mechanism of ammonia transport by Amt/MEP/Rh: structure of AmtB at 1.35 Å. *Science* **305**: 1587–1594.
- Ljungstrom, E., Yates, M.G., and Nordlund, S. (1989) Purification of the activating enzyme for the Fe-protein of nitrogenase from *Azospirillum brasilense*. *Biochim Biophys Acta* **994**: 210–214.
- Lorenz, M.C., and Heitman, J. (1998) The MEP2 ammonium permease regulates pseudohyphal differentiation in *Saccharomyces cerevisiae*. *EMBO J* **17**: 1236–1247.
- Maheswaran, M., Urbanke, C., and Forchhammer, K. (2004) Complex formation and catalytic activation by the PII signaling protein of N-acetyl-L-glutamate kinase from *Synechococcus elongatus* strain PCC 7942. *J Biol Chem* **279**: 55202–55210.
- Martin, D.E., and Reinhold-Hurek, B. (2002) Distinct roles of PII-like signal transmitter proteins and *amtB* in regulation of *nif* gene expression, nitrogenase activity, and posttranslational modification of NifH in *Azoarcus* sp. strain BH72. *J Bacteriol* **184**: 2251–2259.
- Merrick, M., Javelle, A., Durand, A., Severi, E., Thornton, J., Avent, N.D., et al. (2006) The *Escherichia coli* AmtB protein as a model system for understanding ammonium transport by Amt and Rh proteins. *Transfus Clin Biol* **13**: 97–102.
- Ninfa, A.J., and Jiang, P. (2005) PII signal transduction proteins: sensors of alpha-ketoglutarate that regulate nitrogen metabolism. *Curr Opin Microbiol* **8**: 168–173.
- Pedrosa, F.O., and Yates, M.G. (1984) Regulation of nitrogen fixation (*nif*) genes of *Azospirillum brasilense* by *nifA* and *ntr (gln)* type gene products. *FEMS Microbiol Lett* **23**: 95–101.
- Ruppert, U., Irmeler, A., Kloft, N., and Forchhammer, K. (2002) The novel protein phosphatase PphA from *Synechocystis* PCC 6803 controls dephosphorylation of the signalling protein PII. *Mol Microbiol* **44**: 855–864.
- Saari, L.L., Triplett, E.W., and Ludden, P.W. (1984) Purification and properties of the activating enzyme for iron protein of nitrogenase from the photosynthetic bacterium *Rhodospirillum rubrum*. *J Biol Chem* **259**: 15502–15508.
- Schutt, H., and Holzer, H. (1972) Biological function of the ammonia-induced inactivation of glutamine synthetase in *Escherichia coli*. *Eur J Biochem* **26**: 68–72.
- Senior, P.J. (1975) Regulation of nitrogen metabolism in *Escherichia coli* and *Klebsiella aerogenes*: studies with the continuous culture technique. *J Bacteriol* **123**: 407.
- Singleton, C.K., Kirsten, J.H., and Dinsmore, C.J. (2006) Function of ammonium transporter A in the initiation of culmination of development in *Dictyostelium discoideum*. *Eukaryot Cell* **5**: 991–996.
- Strosser, J., Ludke, A., Schaffer, S., Kramer, R., and Burkovski, A. (2004) Regulation of GlnK activity: modification, membrane sequestration and proteolysis as regulatory principles in the network of nitrogen control in *Corynebacterium glutamicum*. *Mol Microbiol* **54**: 132–147.
- Tremblay, P., Drepper, T., Masepohl, B., and Hallenbeck, P.C. (2007) Membrane sequestration of PII proteins and nitrogenase regulation in the photosynthetic bacterium *Rhodobacter capsulatus*. *J Bacteriol* **189**: 5850–5859.
- Wang, H., Franke, C.C., Nordlund, S., and Noren, A. (2005) Reversible membrane association of dinitrogenase reductase activating glycohydrolase in the regulation of nitrogenase activity in *Rhodospirillum rubrum*; dependence on GlnJ and AmtB1. *FEMS Microbiol Lett* **253**: 273–279.
- Winkler, F.K. (2006) Amt/MEP/Rh proteins conduct ammonia. *Pflugers Arch* **451**: 701–707.
- Wolfe, D.M., Zhang, Y., and Roberts, G.P. (2007) Specificity and regulation of interaction between the PII and AmtB1 proteins in *Rhodospirillum Rubrum*. *J Bacteriol* **189**: 6861–6869.
- Xu, Y., Cheah, E., Carr, P.D., van Heeswijk, W.C., Westhoff, H.V., Vasudevan, S.G., and Ollis, D.L. (1998) GlnK, a PII-homologue: structure reveals ATP binding site and indicates how the T-loops may be involved in molecular recognition. *J Mol Biol* **282**: 149–165.
- Xu, Y., Carr, P.D., Huber, T., Vasudevan, S.G., and Ollis, D.L. (2001) The structure of the PII-ATP complex. *Eur J Biochem* **268**: 2028–2037.
- Yakunin, A.F., and Hallenbeck, P.C. (2002) AmtB is necessary for NH₄⁺-induced nitrogenase switch-off and ADP-ribosylation in *Rhodobacter capsulatus*. *J Bacteriol* **184**: 4081–4088.
- Yildiz, O., Kalthoff, C., Raunser, S., and Kuhlbrandt, W. (2007) Structure of GlnK1 with bound effectors indicates regulatory mechanism for ammonia uptake. *EMBO J* **26**: 589–599.

- Zhang, Y., Burris, R.H., Ludden, P.W., and Roberts, G.P. (1997) Regulation of nitrogen fixation in *Azospirillum brasilense*. *FEMS Microbiol Lett* **152**: 195–204.
- Zhang, Y., Wolfe, D.M., Pohlmann, E.L., Conrad, M.C., and Roberts, G.P. (2006) Effect of AmtB homologues on the post-translational regulation of nitrogenase activity in response to ammonium and energy signals in *Rhodospirillum rubrum*. *Microbiol* **152**: 2075–2089.
- Zheng, L., Kostrewa, D., Berneche, S., Winkler, F.K., and Li, X.D. (2004) The mechanism of ammonia transport based on the crystal structure of AmtB of *Escherichia coli*. *Proc Natl Acad Sci USA* **101**: 17090–17095.

Supplementary material

This material is available as part of the online article from:
<http://www.blackwell-synergy.com/doi/abs/10.1111/j.1365-2958.2007.06016.x>
(This link will take you to the article abstract).

Please note: Blackwell Publishing is not responsible for the content or functionality of any supplementary materials supplied by the authors. Any queries (other than missing material) should be directed to the corresponding author for the article.